ADSORPTION PERFORMANCE OF TARTRAZINE BY Cu_xO_y-ZnO COMPOSITE SYNTHESIZED VIA ELECTROCHEMICAL METHOD

ĐÁNH GIÁ KHẢ NĂNG HẤP PHỤ TARTRAZINE CỦA VẬT LIỆU COMPOSITE Cu_xO_y-ZnO TỔNG HỢP BẰNG PHƯƠNG PHÁP ĐIỆN HÓA

Vu Nhat Anh[1], Tran Quoc Toan[1], Pham Hong Chuyen[1], Pham Hoai Linh[2], Duong Thi Tu Anh[1], Nguyen Quoc Dung[1,*]

DOI: http://doi.org/10.57001/huih5804.2025.185

ABSTRACT

In this study, a Cu_xO_y/ZnO (CZO) composite was synthesized and evaluated for the adsorption of tartrazine (TA), a common azo dye in food and industrial applications. The effects of various parameters including pH, contact time, adsorbent dosage, and initial dye concentration were systematically investigated. The adsorption efficiency reached over 96% at pH 5 with 0.015g of CZO for 50mL of 100mg/L TA solution, while the maximum specific adsorption capacity exceeded 500mg/g at higher dye concentrations. Equilibrium was achieved after 90 minutes. Experimental data were fitted to four isotherm models, among which the Freundlich model gave the best correlation ($R^2 = 0.9802$), with $n = 3.68$ indicating favorable multilayer adsorption on a heterogeneous surface. The Langmuir model also showed good agreement ($q_{max} = 520.83$mg/g, $R^2 = 0.9532$), suggesting the presence of localized monolayer adsorption. Kinetic analysis revealed that the pseudo-second-order model provided the best fit ($R^2 = 0.9998$), indicating that chemisorption played a dominant role. These findings highlight the potential application of CZO as an effective and low-cost adsorbent for dye removal from wastewater.

Keywords: *Cu_xO_y-ZnO composite, electrochemical synthesis, Tartrazine adsorption, isotherm models.*

TÓM TẮT

Vật liệu composite Cu_xOy-ZnO (CZO) đã được tổng hợp thành công bằng phương pháp điện hóa và khảo sát khả năng hấp phụ thuốc nhuộm tartrazine trong môi trường nước. Các vật liệu nghiên cứu bao gồm hệ C0 (chỉ chứa Cu_xO_y), Z0 (chỉ chứa ZnO) và CZn (vật liệu composite). Hình thái bề mặt, cấu trúc tinh thể và diện tích bề mặt riêng của vật liệu đã được phân tích để đánh giá đặc tính của vật liệu tổng hợp. Kết quả nghiên cứu cho thấy CZ3 có hiệu suất hấp phụ cao nhất ở pH = 5, với dung lượng hấp phụ cực đại (qmax) đạt 526,3mg/g. Cơ chế hấp phụ được phân tích dựa trên các mô hình đẳng nhiệt và động học, khẳng định tiềm năng ứng dụng của vật liệu trong xử lý nước thải chứa thuốc nhuộm azo. Bên cạnh khả năng hấp phụ cao đối với tartrazine, vật liệu CZn còn cho thấy tiềm năng trong việc loại bỏ nhiều loại chất màu khác khỏi dung dịch nước, góp phần phát triển các công nghệ xử lý ô nhiễm bền vững.

Từ khóa: *Composite Cu_xO_y-ZnO, tổng hợp điện hóa, hấp phụ Tartrazine, mô hình đẳng nhiệt, xử lý nước thải*

[1]Faculty of Chemistry, Thai Nguyen University of Education, Vietnam
[2]Institute of Materials Science, Vietnam Academy of Science and Technology, Vietnam
[*]Email: dungnq@tnue.edu.vn
Received: 19/02/2025
Revised: 21/5/2025
Accepted: 28/5/2025

1. INTRODUCTION

Environmental pollution has become an increasing threat to life on Earth, directly affecting human health and the quality of life. In Vietnam, the rapid pace of industrialization, urbanization, and population growth has placed immense pressure on the environment. Untreated waste from industrial zones and residential areas has significantly contributed to the pollution of soil, water, and air. Among the pollutants, dyes are one of the major contributors, originating from industries such as

textiles, food processing, paper, paints, and pharmaceuticals [1]. These dyes are often discharged directly into wastewater without adequate treatment, causing serious environmental and aesthetic concerns. The discharge of dye-contaminated effluents poses a substantial risk to aquatic life and disrupts ecosystems by altering the physical and chemical properties of the receiving waters. Additionally, the persistence and toxicity of many synthetic dyes complicate their removal, requiring the development of more efficient and sustainable treatment technologies.

Dyes are generally classified based on their dissociation behavior in aqueous media into three main groups: anionic (including azo, acid, direct, and reactive dyes), cationic (basic dyes), and non-ionic (disperse dyes) [2]. Among these, azo dyes are the most widely used, accounting for over half of the dyes present in textile wastewater [3]. Their removal poses significant challenges due to the presence of sulfonate groups, which enhance the dye's polarity and water solubility, making them difficult to adsorb onto non-polar surfaces like activated carbon. Furthermore, the degradation of azo dyes can generate aromatic amines, which are toxic and must be eliminated, adding to the complexity of the treatment process [4]. Tartrazine (marketed as E102 and denoted as TA in this study) is a typical azo dye widely used as a food additive in products such as flavored beverages, energy drinks, bread, chips, sweetened creams, chewing gum, gelatin, yogurt, and also in pharmaceutical capsules [5]. In Vietnam, tartrazine is commonly found in popular dishes such as "salt-baked chicken" and various processed foods. Despite its extensive use, tartrazine has been linked to several adverse health effects, including allergies, asthma, hyperactivity, genotoxicity, carcinogenicity, eczema, and immunosuppression [6]. As a result, tartrazine can easily enter the environment through domestic wastewater, posing significant risks to aquatic ecosystems and human health. Consequently, the need for effective methods to remove tartrazine from contaminated water has become an urgent environmental challenge. Among existing treatment technologies including oxidation, membrane separation, biological, and coagulation methods adsorption is considered a promising approach due to its simplicity, low cost, and high efficiency even at low dye concentrations. Nevertheless, the adsorption performance strongly depends on the properties of the adsorbent material.

Recently, nanomaterials based on transition metal oxides such as CuO, ZnO [7, 8], and their composites have attracted attention due to their large surface area, high surface activity, and potential for chemical interactions with azo dyes. In this study, we investigate the adsorption behavior of a CZO composite, synthesized via a electrochemical method, for the removal of tartrazine from aqueous solution. The incorporation of ZnO into copper oxides is expected to enhance adsorption efficiency by increasing the number of active sites, improving microstructure, and strengthening interactions with the sulfonate groups of tartrazine.

2. EXPERIMENTAL

2.1. Chemicals and Equipment

High-purity copper metal (99.7%); zinc sulfate heptahydrate ($ZnSO_4 \cdot 7H_2O$, 99.5%, Merck KGaA, Germany); sodium hydroxide (NaOH, 99.5%, Merck KGaA, Germany); glucose monohydrate ($C_6H_{12}O_6 \cdot H_2O$, 99.5%, Merck KGaA, Germany); tartrazine powder (Indonesia); and double-distilled water were used throughout the experiments.

2.2. Synthesis of Materials

The CZO composite material (abbreviated as CZO) was synthesized via a simultaneous electrochemical and solution-phase method, as previously described in the group's earlier study [9]. In this process, copper-containing species were generated by anodic dissolution of copper, while ZnO was formed in solution from the $ZnSO_4$ precursor. The resulting material exhibited a porous structure, nanoscale particle size, and high dispersion. Among the synthesized samples, the composite with a suitable Zn content (coded as CZ3) was selected for adsorption experiments involving tartrazine. To evaluate the structural and morphological features of the synthesized material, a series of characterization techniques were employed. The surface morphology and internal nanostructure were examined using field-emission scanning electron microscopy (FESEM) and transmission electron microscopy (TEM). Phase identification and crystallinity were investigated by X-ray diffraction (XRD). Nitrogen adsorption–desorption analysis was conducted to determine surface area, pore volume, and pore size distribution, based on BET and BJH methods.

2.3. Adsorption Studies

The adsorption performance of the CZO composite was evaluated by batch adsorption experiments using

aqueous tartrazine solutions. After a defined contact time, the solution was filtered, and the residual tartrazine concentration was determined by UV-Vis spectrophotometry at the maximum absorption wavelength of λ = 427nm.

2.3.1. Adsorption Capacity and Removal Efficiency

The removal efficiency (%) and the adsorption capacity at equilibrium, (q_e: mg/g) were calculated using the following equations:

$$\text{Removal}\ (\%) = \frac{C_0 - C_t}{C_0} \times 10 \quad (1)$$

$$q_e = \frac{(C_0 - C_e)V}{m} \quad (2)$$

where C_0 and C_e (mg/L) are the initial and equilibrium concentrations of tartrazine (TA), respectively; V (L) is the solution volume, and m (g) is the mass of the adsorbent. The effects of various parameters such as solution pH, initial tartrazine concentration, contact time, temperature, and adsorbent dosage were individually investigated to determine the optimal adsorption conditions.

2.3.2. Adsorption Kinetics Models

To understand the mechanism and rate of tartrazine adsorption onto the CZO composite, experimental data as a function of time were fitted to four commonly used kinetic models: pseudo-first-order, pseudo-second-order, Elovich, and intraparticle diffusion. Each model represents distinct aspects of the adsorption mechanism.

Table 1. Summary of linear forms and characteristic parameters of adsorption kinetic models used to describe the tartrazine adsorption process onto CZO

Model	Linear Equation	Characteristic parameters
Pseudo-first-order	$\ln(q_e - q_t) = \ln q_e - k_1 t$	k_1: rate constant (min^{-1})
Pseudo-second-order	$\frac{t}{q_t} = \frac{1}{k_2 q_e^2} + \frac{1}{q_e} t$	k_2: rate constant ($g.mg^{-1}min^{-1}$)
Elovich	$q_t = \frac{1}{\beta}\ln(\alpha\beta) + \frac{1}{\beta}\ln t$	α initial adsorption rate ($g.mg^{-1}min^{-1}$); β: activation-related constant (g/mg).
Intraparticle diffusion	$q_t = k_{id}.t^{0.5} + C$	k_{id}: intraparticle diffusion rate constant ($mg.g^{-1}.min^{0.5}$).

In the Table 1, q_t and q_e represent the amount of adsorbed tartrazine at time t and at equilibrium (mg/g), respectively, and ttt is the contact time (min)

2.3.3. Adsorption Isotherm Models

To gain insight into the nature of the interaction between tartrazine and the CZO surface, equilibrium adsorption data were fitted to four isotherm models: Langmuir, Freundlich, Temkin, and Dubinin-Radushkevich (D-R). These models help identify whether the adsorption process is monolayer or multilayer, homogeneous or heterogeneous, and physical or chemical in nature.

Table 2. Linear equations and key parameters of isotherm models applied to interpret the equilibrium adsorption behavior of tartrazine on the CZO surface

Model	Linear Form	Characteristic Parameters
Langmuir	$\frac{C_e}{q_e} = \frac{1}{q_{max}K_L} + \frac{C_e}{q_{max}}$	q_{max}: maximum adsorption capacity (mg/g), K_L: Langmuir constant (L/mg)
Freundlich	$\ln q_e = \ln K_F + \frac{1}{n}\ln C_e$	K_F: adsorption capacity constant, n: là adsorption intensity
Temkin	$q_e = \frac{RT}{b_T}\ln K_T + \frac{RT}{b_T}\ln C_e$	K_T: Tempkin constant, $\frac{RT}{b_T}$ related to heat of adsorption
Dubinin–Radushkevich	$\ln q_e = \ln q_{max} - \beta\varepsilon^2$	q_{max}: maximum adsorption capacity (mg/g), β: D-R constant, $\varepsilon = RT\ln(1 + \frac{1}{C_e})$

In the Table 2, q_e is the amount of tartrazine adsorbed at equilibrium (mg/g); C_e is the equilibrium concentration of tartrazine (mg/L), R is the universal gas constant (8.314J/mol·K); T is the absolute temperaturei (K); ε is the Polanyi potentia, b_T reflects the adsorption energy interaction between adsorbate and adsorbent surface.

3. RESULTS AND DISSCUSION

3.1. Morphological and structural characteristics of CZO material

The morphology of the CZO composite observed from SEM (Figure 1a) reveals a rough, flower-like and aggregated nanostructure, which provides high surface exposure. TEM image (Figure 1b) further confirms the presence of spherical and rod-shaped particles with sizes typically below 100 nm. The XRD pattern (Figure 1c) indicates that the material consists of a mixture of Cu_2O,

Cu, and ZnO crystalline phases, with broad peaks suggesting nanocrystalline domains. The UV-Vis DRS spectrum (Figure 1d) shows broad absorption in the visible region, and the Tauc plot (Figure 1e) yields an estimated direct bandgap of 1.70 eV. This narrowed bandgap is attributed to the interaction between Cu and Zn oxides, potentially enhancing the material's performance in visible-light-assisted applications.

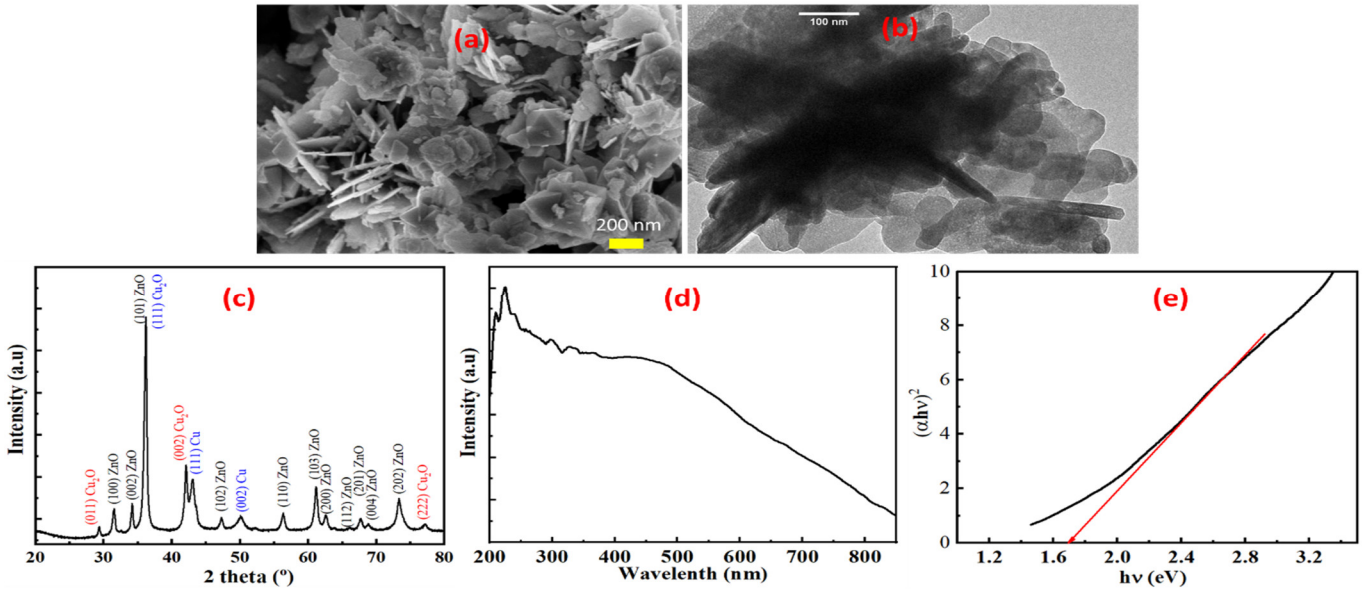

Figure 1. Structural and physicochemical characterization of the CZO composite: (a) SEM image; (b) TEM imag; (c) XRD pattern; (d) UV–Vis DRS; (e) Tauc plot used to estimate the optical bandgap assuming direct transition

Figure 2a illustrates the nitrogen adsorption-desorption isotherm of the CZO composite at 77K, which exhibits a type IV isotherm with a clear hysteresis loop in the high relative pressure region (P/P_0 > 0.8). This indicates a mesoporous structure, which is highly desirable for facilitating molecular diffusion and adsorption processes. The shape and loop type suggest the presence of slit- or ink-bottle-like pores, commonly found in aggregated nanostructures.

Figure 2b, showing the incremental pore volume (dV/dD) distribution, confirms that the majority of pore volume arises from pores within the 3 - 20nm range. This size range is particularly effective for adsorbing organic molecules such as tartrazine, as it allows rapid diffusion and large adsorption capacity. The total pore volume, as summarized in Table 3, reaches approximately 0.031cm^3/g, reflecting the high porosity of the material.

Figure 2c presents the incremental pore area (dA/dD) distribution, where the maximum surface area contribution originates from pores in the range of 3 - 8nm. This finding indicates that these mesopores are not only abundant but also offer a large accessible surface area for adsorption. The cumulative surface area reaches ~7.7m^2/g, which is consistent with the BET surface area of 8.21m^2/g obtained via nitrogen adsorption.

These results together provide strong evidence that the CZO composite possesses a mesoporous structure with well-distributed pore sizes, significant surface area, and adequate pore volume all of which contribute directly to its efficient adsorption behavior, especially in the context of environmental dye removal such as tartrazine.

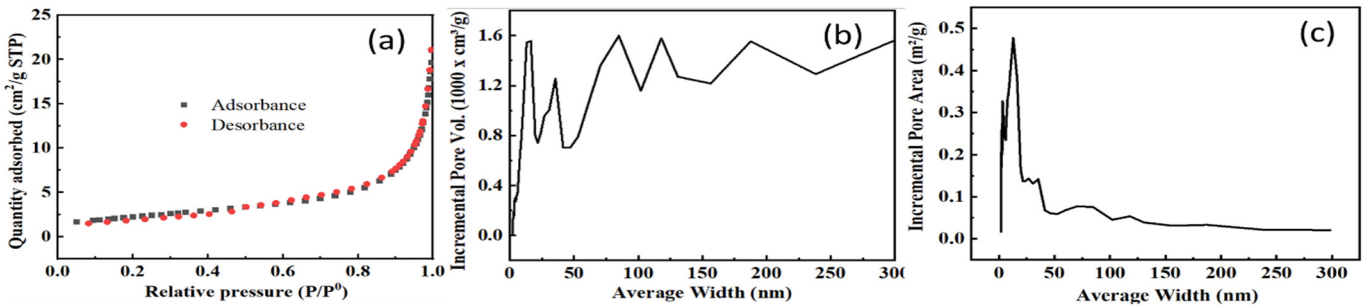

Figure 2. (a) Nitrogen adsorption–desorption isotherm of the CZO composite recorded at 77 K; BJH pore size distribution in terms of incremental pore volume (dV/dD); and (c) Incremental pore area (dA/dD)

Table 3. Textural parameters of the CZO composite determined by BET and BJH analyses

Parameter	Value
BET surface area	8.21m^2/g
BJH adsorption pore volume	0.0310cm^3/g
BJH average pore diameter (ads/des)	16.07/16.63nm
BJH surface area (ads/des)	7.72/8.22m^2/g
DH pore diameter (ads/des)	15.43/15.29nm

3.2. Tartrazine adsorption properties of materials

3.2.1. Determination of the Point of Zero Charge and Effect of pH on Adsorption Capacity

The point of zero charge pH_{iep} is a critical parameter for evaluating the surface characteristics of an adsorbent, particularly its electrostatic interaction with charged species in aqueous solutions. The pH_{iep} of the denoted as CZO was determined by immersing 0.01g of the material in 100mL of 0.1M NaCl solution adjusted to different initial pH values pH_i. After 48 hours of agitation, the final pH_f was measured. A plot of pH_i - pH_f versus pH_i is shown in Figure 3a. The curve intersects the horizontal axis at approximately pH ≈ 7.9, indicating that the pH_{iep} of the CZO material is 7.9. Below this pH, the surface of the material becomes positively charged due to protonation of surface hydroxyl groups; above this value, the surface becomes negatively charged as deprotonation occurs. To investigate the effect of pH on adsorption performance, batch adsorption experiments were conducted using 0.01g of CZO in 50 mL of 100 mg/L tartrazine (TA) solution at various pH levels ranging from 3 to 9. As shown in Figure 3b, the adsorption efficiency was highest (> 85%) at pH 3 - 5 and significantly decreased as the pH increased, especially in the range of pH 6 - 7, reaching very low efficiency at pH > 8. The strong dependence of adsorption efficiency on pH can be attributed to electrostatic interactions between the CZO surface and tartrazine molecules. At pH_{iep} the positively charged surface facilitates electrostatic attraction with the sulfonate groups ($-SO_3^-$) of TA, which carries a negative charge in aqueous solution. Conversely, when the pH exceeds the pH_{iep}, the CZO surface becomes negatively charged, resulting in electrostatic repulsion with TA molecules, thus reducing adsorption efficiency.However, at excessively low pH (e.g., pH = 3), the material may undergo partial dissolution or degradation of active adsorption sites. Therefore, pH = 5 was selected as the optimal condition for subsequent adsorption experiments, offering a compromise between high adsorption efficiency and chemical stability of the material.

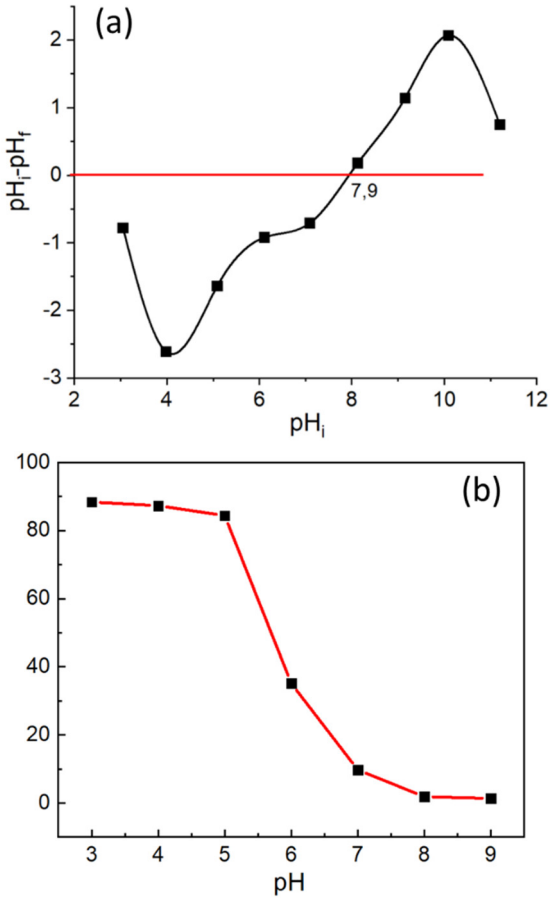

Figure 3. (a) Determination of isoelectric point of CZO material; (b) Effect of pH on adsorption capacity of CZO material

3.2.2. Effect of time on tartrazine adsorption

To determine the time required to reach adsorption equilibrium, experiments were carried out by adding 0.01 g of CZO to 50mL of tartrazine (TA) solution with an initial concentration of 100mg/L at pH 5, under agitation at 350rpm. Samples were collected at various time intervals (0, 15, 30, 60, 90, 120, and 150 minutes) and analyzed using UV-Vis spectrophotometry.

The results are presented in Figure 4. The absorbance at the characteristic wavelength of TA (~427nm) decreased significantly with increasing contact time (Figure 4a), indicating a marked reduction in TA concentration due to adsorption onto the CZO surface. The adsorption efficiency (H%) increased rapidly within the first 30 minutes, reaching approximately 70%, then gradually leveled off and approached equilibrium after 60 minutes. After 90 minutes, only slight changes in TA concentration were observed, suggesting that

equilibrium had been reached (Figure 4b). Therefore, a contact time of 90 minutes was selected as the optimal adsorption duration for subsequent experiments.

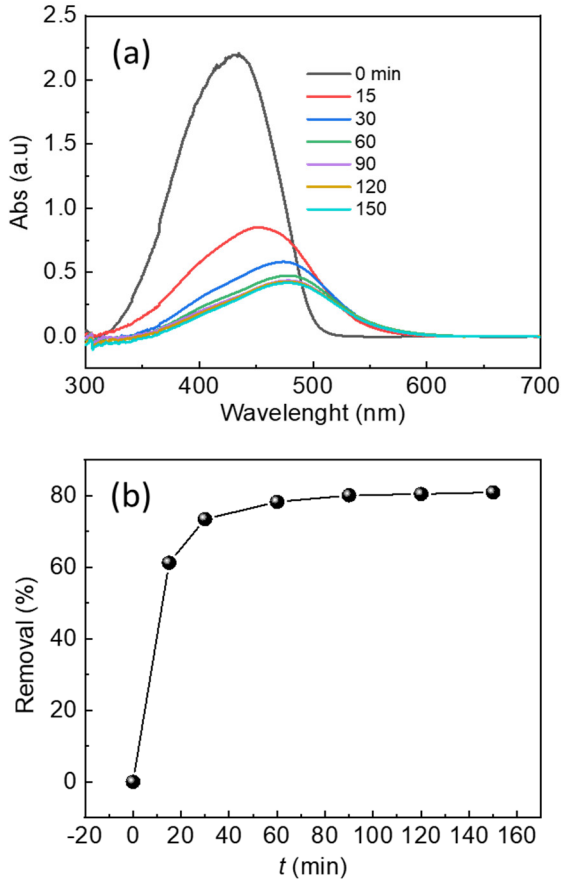

Figure 4. (a) UV-Vis absorption spectra of tartrazine solution during adsorption by CZO at different contact times (0 - 150 min); (b) Variation of adsorption efficiency (H%) as a function of contact time.

3.2.3. Effect of Adsorbent Dosage

The influence of adsorbent dosage on the removal efficiency of tartrazine (TA) was investigated using different amounts of CZO. Batch adsorption experiments were conducted with 50mL of 100mg/L TA solution at pH 5, under agitation at 350rpm for 90 minutes. The mass of CZO was varied from 0.005g to 0.04g. As shown in Figure 5b, the adsorption efficiency (H%) increased from approximately 75% to over 88% when the amount of CZO increased from 0.005g to 0.04g. This enhancement is attributed to the greater number of available active sites on the surface of the adsorbent, facilitating more interactions with TA molecules in solution. However, beyond 0.02g, the increase in efficiency became less pronounced, indicating a tendency toward saturation.

Conversely, the adsorption capacity per unit mass of adsorbent (q_t , mg/g) decreased with increasing dosage, from around 750mg/g at 0.005g to approximately 250mg/g at 0.04g. This decline can be explained by the fixed initial pollutant concentration; while more TA is removed in total, the amount adsorbed per gram of material is reduced. Additionally, particle aggregation and overlapping at higher dosages may lead to a reduction in the number of accessible adsorption sites.

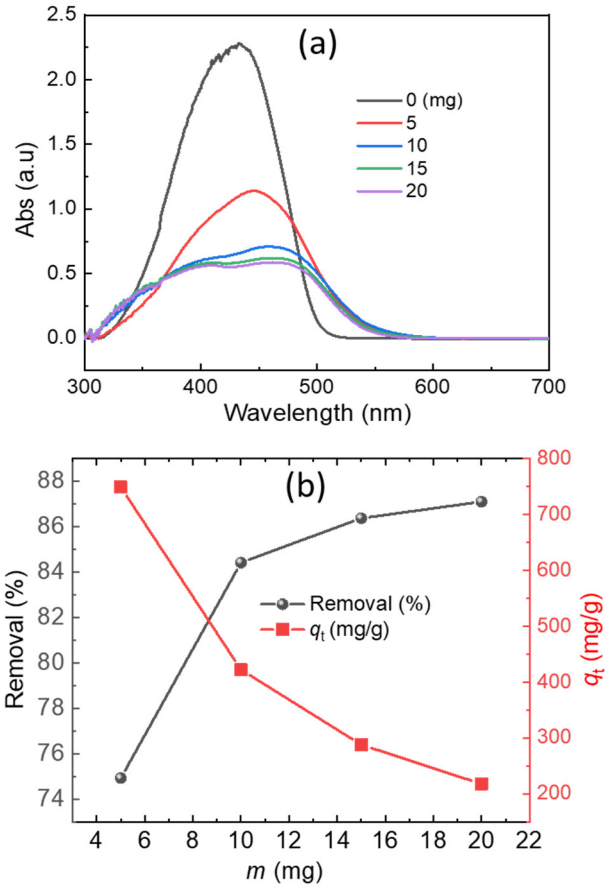

Figure 5. (a) Effect of CZO dosage on the specific adsorption capacity q_t of tartrazine; (b) Variation of adsorption efficiency (H%) with increasing adsorbent mass

3.2.4. Effect of Initial TA Concentration

To investigate the influence of initial tartrazine (TA) concentration on the adsorption performance of CZO, batch experiments were conducted using a fixed amount of adsorbent (0.015g) in 50mL of TA solution with varying initial concentrations ranging from 50 to 250mg/L. The experiments were performed at pH 5, under agitation at 350rpm for 90 minutes. The results are presented in Figure 6. As the initial TA concentration increased from 50mg/L to 250mg/L, the adsorption efficiency (H%) decreased from approximately 96% to ~58%, while the specific adsorption capacity (q_t, mg/g) increased from ~180mg/g to over 500mg/g. This behavior can be explained as follows: At low concentrations, TA molecules are relatively scarce and can easily access and occupy the

available active sites on the CZO surface, resulting in high removal efficiency. At higher concentrations, the number of TA molecules exceeds the number of available adsorption sites, leading to a reduction in removal efficiency. However, the overall amount of TA adsorbed still increases, contributing to a higher q_t. In addition, increasing the initial TA concentration enhances the driving force for mass transfer from the solution to the adsorbent surface, which further contributes to the increase in adsorption capacity. Nevertheless, due to the finite number of active sites, the efficiency cannot continue to rise indefinitely. These results suggest that an appropriate initial concentration must be selected to optimize both adsorption efficiency and capacity. A concentration range of 100 - 150mg/L was deemed suitable for further isotherm and mechanistic studies.

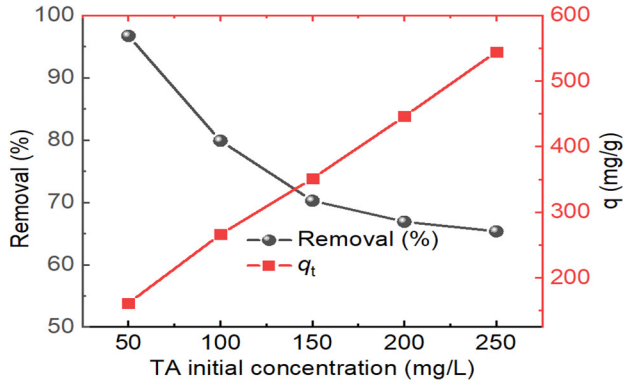

Figure 6. (a) Adsorption efficiency (H%) of CZO at different initial tartrazine (TA) concentrations; (b) Variation of specific adsorption capacity (q_t) with initial TA concentration

3.2.5. Adsorption Kinetics

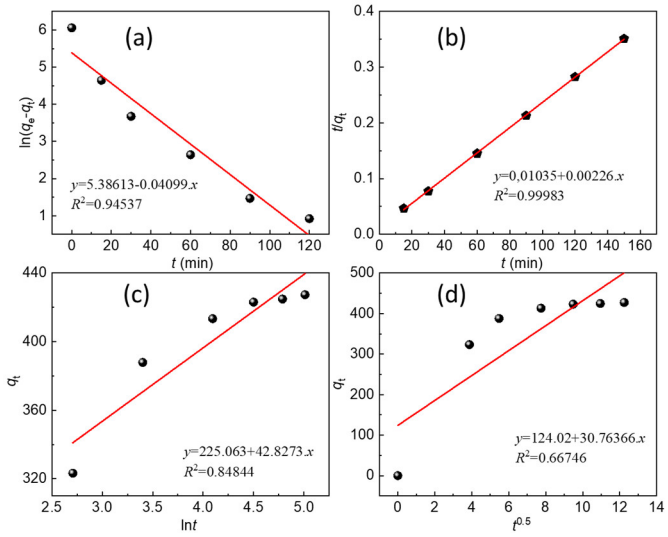

Figure 7. Linearized kinetic models for tartrazine adsorption onto CZO: (a) pseudo-first-order (PFO), (b) pseudo-second-order (PSO), (c) Elovich, and (d) intraparticle diffusion

Based on the dependence of adsorption capacity on contact time, several kinetic models were applied to describe the adsorption process, including the pseudo-first-order (PFO), pseudo-second-order (PSO), Elovich, and intraparticle diffusion models. The linearized forms of these kinetic equations were fitted to the experimental data, and the corresponding plots are presented in Figure 7.

The kinetic parameters derived from fitting the four models are summarized in Table 4. Among them, the pseudo-second-order model exhibited the best fit to the experimental data. The good agreement with the pseudo-second-order model suggests that the adsorption rate is governed not only by the concentration of tartrazine but also by the interaction potential between the adsorbate molecules and the adsorbent surface an indication typically associated with chemisorption mechanisms.

Table 4. Kinetic parameters of tartrazine adsorption fitted by pseudo-first-order, pseudo-second-order, Elovich, and intraparticle diffusion models

Model	Slope	Intercept	R^2
Pseudo-first-order	-0.04099	5.38613	0.94537
Pseudo-second-order	0.00226	0.01035	**0.99983**
Elovich	42.8273	225.063	0.8788
Intraparticle diffusion	30.7637	124.02	0.66746

3.2.6. Adsorption Isotherm Models

The linearized forms of the Langmuir, Freundlich, Temkin, and Dubinin-Radushkevich (D-R) isotherm models were applied and are presented in Figure 8. The corresponding parameters obtained from these models are summarized in Table 5. According to the Langmuir model, the maximum adsorption capacity q_{max} was 520.83mg/g, with a Langmuir constant K_L = 11.30L/mg and a correlation coefficient R^2 = 0.9532 suggesting a good fit to the experimental data. This indicates that the adsorption process may occur on a relatively homogeneous surface and follows a monolayer adsorption mechanism.

For the Freundlich model, the constants were found to be K_F = 11.30, n = 3.6785 and R^2 = 0.9802. Since n > 1, the adsorption is considered favorable. Moreover, the highest R^2 value among the tested models indicates that the Freundlich model provides the best fit for the system under study. The Temkin model accounts for adsorbate-adsorbent interactions and assumes that the adsorption energy decreases linearly with increasing surface coverage. The calculated Temkin binding energy b_T =

32.168J/mol falls within the range of 20 - 80J/mol, suggesting that the adsorption mechanism involves either weak chemisorption or strong physisorption. However, the model's correlation coefficient R^2 = 0.9228 lower than that of the Langmuir and Freundlich models.

In the Dubinin-Radushkevich model, the maximum adsorption capacity q_{max} was 1165mg/g and the mean adsorption energy *E* = 15.656kJ/mol. Since the value of E lies within the range of 8 - 16kJ/mol and is less than 20kJ/mol, it suggests that the adsorption process is predominantly physical in nature, likely governed by weak interactions such as van der Waals forces or hydrogen bonding between tartrazine molecules and the functional groups on the CZO surface. This also implies the potential reusability of the material, as its structure may not be significantly altered after adsorption. Based on the correlation coefficients and model parameters, the Freundlich model exhibited the best fit, suggesting that tartrazine adsorption on CZO occurs on a heterogeneous surface and follows a multilayer adsorption mechanism. Nevertheless, the relatively good fit of the Langmuir model and the energy values derived from the D-R model also point to the involvement of chemical adsorption and the possibility of partial monolayer formation.

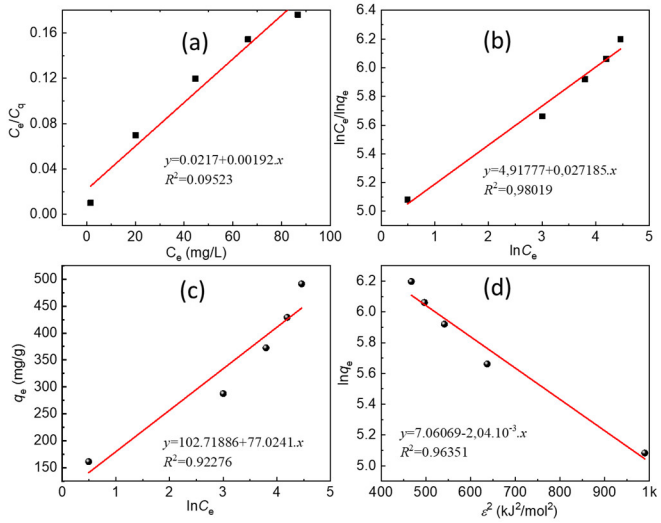

Figure 8. Linearized adsorption isotherms for tartrazine on CZO: (a) Langmuir, (b) Freundlich, (c) Temkin, and (d) Dubinin-Radushkevich models

In comparison with other adsorbents previously reported for tartrazine removal, the CZO composite exhibited a significantly higher adsorption capacity. As summarized in Table X, the maximum adsorption capacity q_t of CZO reached 526.3mg/g based on the Langmuir model. This value far exceeds that of many conventional and modified materials, such as commercial biochar: 3.26mg/g [10], positively charged triethylenetetramine biochar: 85.47 (mg/g) [11], bromide-modified bentonite 175.80 and 201.00 (mg/g) [12], activated sawdust: 127 (mg/g) [13], and chitosan/polyaniline 584.00 (mg/g) [14]. The outstanding adsorption capacity can be attributed to the synergistic effect between copper and zinc oxides, providing a large number of active sites and facilitating electrostatic and chemical interactions with sulfonate groups of tartrazine. These results suggest that CZO is not only a highly efficient adsorbent but also a competitive candidate among both natural and engineered materials for practical wastewater treatment applications.

Table 5. Adsorption parameters obtained from isotherm models

Model	Slope	Intercept	R^2	Parameter 1	Parameter 2
Langmuir	0.00192	0.0217	0.95323	q_{max} = 520.83 mg/g	K_L = 11.30
Freundlich	0.27185	4.91777	0.98019	n = 3.6785	K_F = 11.3
Temkin	77.0241	102.71886	0.92276	$\frac{RT}{b_T}\ln K_T$ = 102.72 K_T = 3.796 (L/g)	$\frac{RT}{b_T}$ = 77.02 b_T = 32.168J/mol
Dubinin-Radushkevich	0.00204	7.06069	0.9635	q_{max} = 1165mg/g	15.656kJ/mol

4. CONCLUSION

The synthesized CZO composite demonstrated excellent adsorption performance for tartrazine, with maximum removal efficiency exceeding 96% and specific adsorption capacity reaching over 500mg/g under optimized conditions. Adsorption equilibrium was attained within 90 minutes, suggesting rapid interaction between dye molecules and active sites on the adsorbent surface. Kinetic analysis confirmed that the pseudo-second-order model best described the process (R^2 = 0.9998), indicating that chemisorption dominated the adsorption mechanism. Isotherm studies revealed that the Freundlich model had the highest correlation (R^2 = 0.9802), suggesting multilayer adsorption on a heterogeneous surface, while the Langmuir model also showed good fit with a theoretical q_{max} of 520.83mg/g. These results demonstrate that CZO is a promising adsorbent for the efficient removal of azo dyes from aqueous solutions, combining high capacity, fast kinetics, and the potential for practical wastewater treatment applications.

REFERENCES

[1]. L. Bulgariu, L. B. Escudero, O. S. Bello, M. Iqbal, J. Nisar, K. A. Adegoke, F. Alakhras, M. Kornaros, I. Anastopoulos, "The utilization of leaf-based adsorbents for dyes removal: A review," *Journal of Molecular Liquids,* 276, 728-747, 2019.

[2]. S. M. Prabhu, A. Khan, M. H. Farzana, G. C. Hwang, W. Lee, G. Lee, "Synthesis and characterization of graphene oxide-doped nano-hydroxyapatite and its adsorption performance of toxic diazo dyes from aqueous solution," *Journal of Molecular Liquids,* 269, 746-754, 2018.

[3]. I. K. Konstantinou, T. A. Albanis, "TiO_2-assisted photocatalytic degradation of azo dyes in aqueous solution: kinetic and mechanistic investigations: A review," *Applied Catalysis B: Environmental,* 49, 1, 1-14, 2004.

[4]. J. Sokolowska-Gajda, H. S. Freeman, A. Reife, "Synthetic dyes based on environmental considerations. Part 2: Iron complexes formazan dyes," *Dyes and pigments,* 30, 1, 1-20, 1996.

[5]. M. Wawrzkiewicz, Z. Hubicki, "Removal of tartrazine from aqueous solutions by strongly basic polystyrene anion exchange resins," *Journal of Hazardous Materials,* 164, 2-3, 502-509, 2009.

[6]. S. Banerjee, M. Chattopadhyaya, "Adsorption characteristics for the removal of a toxic dye, tartrazine from aqueous solutions by a low cost agricultural by-product," *Arabian Journal of Chemistry,* 10, S1629-S1638, 2017.

[7]. L. T. Dat, N. T. Hung, V. A. Tuan, "Preparation of flower-like Cu_2O/ZnO for removal of dyes from aqueous medium," *Vietnam Journal of Chemistry,* 58, 4, 517-525, 2020.

[8]. J. D. Dai, L. Gan, H. Y. Zhang, C. M. Liu, "The decoloration of anionic and cationic dyes using ZnO and ZnO-Cu_2O," *Crystals,* 9, 5, 229, 2019.

[9]. Ha Xuan Linh, Nguyen Quoc Dung, Hoai Linh Pham, Nguyen Xuan Hoa, Dang Van Thanh, Tran Thi Kim Ngan, Pham Huong Quynh, Khieu Thi Tam, "One-step electrochemical synthesis of CuxO–ZnO for antifungal activity," *Applied Nanoscience*, 15, 14, 2025.

[10]. M.L. Soran, M. Bocșa, S. Pintea, A. Stegarescu, I. Lung, O. Opriș, "Commercially biochar applied for tartrazine removal from aqueous solutions," *Applied Sciences,* 14, 1, 53, 2023.

[11]. M. E. Mahmoud, A. M. Abdelfattah, R. M. Tharwat, G. M. Nabil, "Adsorption of negatively charged food tartrazine and sunset yellow dyes onto positively charged triethylenetetramine biochar: Optimization, kinetics and thermodynamic study," *Journal of Molecular Liquids,* 318, 114297, 2020.

[12]. S. Sahnoun, M. Boutahala, C. Tiar, A. Kahoul, "Adsorption of tartrazine from an aqueous solution by octadecyltrimethylammonium bromide-modified bentonite: Kinetics and isotherm modeling," *Comptes Rendus. Chimie,* 21, 3-4, 391-398, 2018.

[13]. B. Rzig, R. Kojok, E. B. Khalifa, G. Magnacca, T. Lahssini, B. Hamrouni, N. Bellakhal, "Adsorption performance of tartrazine dye from wastewater by raw and modified biomaterial: Equilibrium, isotherms, kinetics and regeneration studies," *Biomass Conversion and Biorefinery,* 14, 15, 18313-18330, 2024.

[14]. S. Sahnoun, M. Boutahala, "Adsorption removal of tartrazine by chitosan/polyaniline composite: kinetics and equilibrium studies," *International Journal of Biological Macromolecules,* 114, 1345-1353, 2018.

THÔNG TIN TÁC GIẢ

Vũ Nhật Anh[1], Trần Quốc Toàn[1], Phạm Hồng Chuyên[1], Phạm Hoài Linh[2], Dương Thị Tú Anh[1], Nguyễn Quốc Dũng[1]

[1]Khoa Hóa học, Trường Đại học Sư phạm - Đại học Thái Nguyên

[2]Viện Khoa học vật liệu, Viện Hàn lâm Khoa học và Công nghệ Việt Nam